CrossMark

The Impact of Microenvironment on the Synovial Sarcoma Transcriptome

Huifeng Jin[1] · Jared J. Barrott[1] · Matthew G. Cable[1] · Michael J. Monument[1] ·
Daniel M. Lerman[1] · Kyllie Smith-Fry[1] · Dakota Nollner[1] · Kevin B. Jones[1,2]

Abstract Synovial sarcoma (SS) is initiated by a *t(X;18)* chromosomal translocation and resultant *SS18-SSX* fusion oncogene. Only a few SS cell lines exist. None has been compared to its source tumor. In order to compare matched tumor and cell line pairs, we performed RNAseq on 3 tumor/cell line pairs from a genetically engineered mouse model of SS, as well as 2 pairs from human SS tumors. Transcriptomes of mouse tumors and derivative cell lines deviated significantly. Differentially expressed genes highlighted inflammatory infiltrates and metabolism. The same was found for the human tumor and cell line pairs. More was shared between different tumors than between any tumor and its cell line. Direct xenografting generated transcriptomes that more closely resembled the primary tumor than did its derivative cell line. SS tumor transcriptomes are powerfully impacted by the environment wherein they reside, especially with regard to immune interaction and metabolism.

Huifeng Jin and Jared J. Barrott co-first authors

✉ Kevin B. Jones
  kevin.jones@hci.utah.edu

[1] Departments of Orthopaedics and Oncological Sciences, Huntsman Cancer Institute, University of Utah School of Medicine, Salt Lake City, UT, USA

[2] Huntsman Cancer Institute, 2000 Circle of Hope Drive, Room 4263, Salt Lake City, UT 84112, USA

Introduction

Most discovery biology and therapy-evaluating science related to cancer begins in cell lines derived from tumors. The process of developing these cell lines necessarily introduces departures from the biology of the cancer cells in their native tumor environment [1]. Such changes have yet to be extensively studied, despite our reliance on the faithful recapitulation of tumor biology in cell culture models.

As the most common and most deadly soft-tissue sarcoma in the adolescent and young adult population [2], SS merits the development of better therapeutic options, which have not improved in many decades [3]. Driven by *SS18-SSX* fusion genes generated by characteristic *t(X;18)* chromosomal translocations, SS is considered a genome-stable malignancy harboring few other genetic changes [4–6]. There is strong homogeneity, both genetic and histomorphologic among the cells in any given SS [7]. This stability and homogeneity proffer tacit confidence that the biology of derivative cell lines in culture represents SS tumor biology well.

However, SSs have proven difficult to culture, suggesting that the cells that ultimately grow in vitro may have been selected to have many departures from their native biology [8]. We turned to a source of multiplied opportunities for culturing fresh tumors: a genetically engineered mouse model of synovial sarcomagenesis.

Methods

Human Synovial Sarcomas

Human tumors were collected with the approval of the institutional review board from consented patients and in accordance with legal and ethical standards. Each human case was clinically

confirmed to bear the characteristic chromosomal translocation by fluorescent in situ hybridization for the break-apart SS18 probe. Each of the included cases was later confirmed to express the SS18-SSX1 fusion, specifically, by RT-PCR.

Mice

Mouse experiments were conducted with the approval of the institutional animal care committee in accordance with legal and ethical standards. The previously described, $Rosa26^{hSS1};Myf5Cre^{+}$ and $Rosa26^{hSS2};Myf5Cre^{+}$ mice were maintained on a mixed strain background, C57BL/6 and SvJ. Genotyping was performed as previously described [4]. Expression of the fusion was confirmed by expression in each tumor of GFP, which is expressed from the same transcript as each SS18-SSX fusion oncogene. Of the included tumors, M1 and M2 were derived from SS18-SSX1-expressing mice and M3 from an SS18-SSX2-expressing mouse.

Xenografts were initiated by dicing freshly harvested human SSs into 1-2 mm^3 fragments and embedding each subcutaneously into the flank of an NSG mouse.

Transcriptome Analyses

Total RNA was isolated with the RNeasy mini kit (Qiagen, Valencia, CA, USA), prepared using the Illumina TruSeq RNA kit (Illumina, San Diego, CA, USA), checked with the Agilent Bioanalyzer RNA 6000 chip (Agilent Technologies, Santa Clara, CA, USA), captured using the RiboZero method (Illumina), and 50-cycle end-read sequenced on an Illumina HiSeq 2000. Reference fasta files were generated by combining the chromosome sequences from mm10 with all possible splice junction sequences, which were generated with USeq (v8.8.8) MakeTranscriptome using a radius of 46 and annotated with Ensembl transcripts (build 74) from the UCSC browser. Reads were aligned with Novoalign (v2.08.01), allowing up to 50 alignments per read. USeq's SamTranscriptomeParser selected the best alignment for each and converted the coordinates of reads aligning to splices back to genomic space. Differential gene expression was measured using USeq's DefinedRegionDifferentialSeq. Briefly, the number of reads aligned to each gene were calculated, then normalized in DESeq2. R package 'pheatmap' (v1.0.2) generated heatmaps. Log2 (FPKM) values were centered and scaled by gene. Significance was tested with a right tailed Fisher Exact Test and p-value correction according to the Benjamini-Hochberg method for multiple testing [9, 10]. Function Dist in DeSeq2 package in R was used to calculate the Euclidean distance between samples and to provide an overview of similarities and dissimilarities between samples for the hierarchical clustering.

Notably, the RNAseq data from the human xenografts was aligned only to the human genome, making possible the filtering out of transcriptomic contributions from the murine infiltrating inflammatory, stromal, and endothelial cells. However, the human and mouse genomes for coding sequence are sufficiently homologous to make the clear separation between transcripts from these cells very unlikely from 50 bp reads.

Histology

Tissues were fixed in 4% paraformaldehyde overnight, and embedded in paraffin. Paraffin-embedded tissues were stained
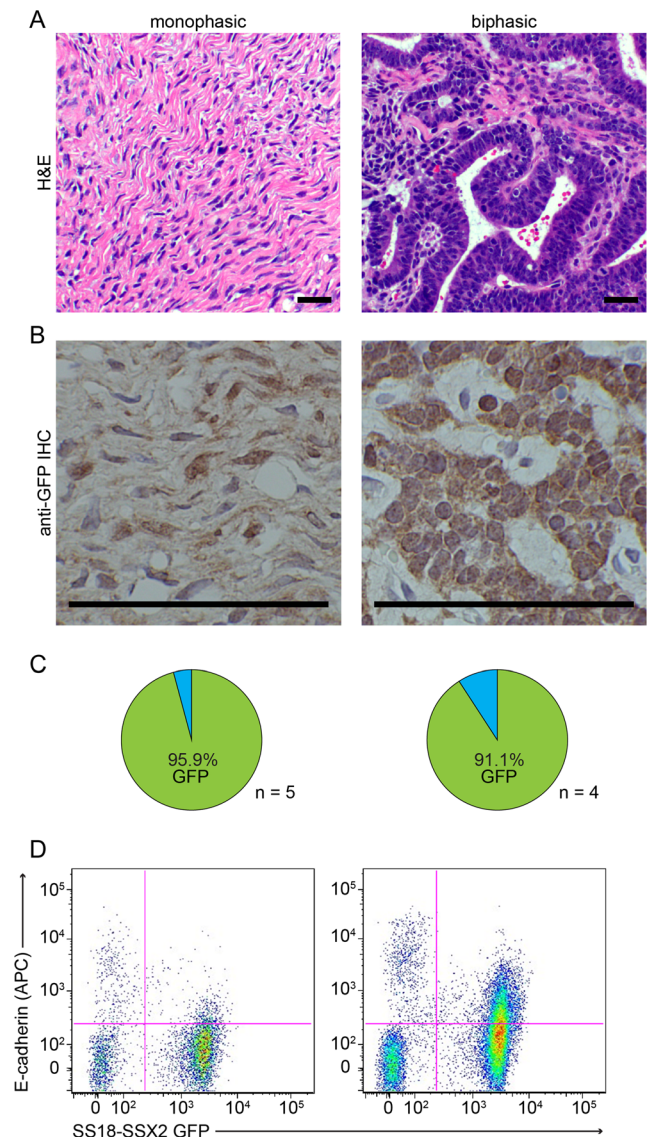
Fig. 1 Synovial sarcomas are comprised of a high percentage of tumor cells. a Photomicrographs of H&E histology examples of monophasic (MSS, *left*) and biphasic (BSS, *right*) SS18-SSX-induced synovial sarcomas from *Myf5Cre*-induced mice. b Photomicrographs following immunohistochemistry against GFP in MSS (left) and BSS (*right*) synovial sarcomas. c Pie charts demonstrating the percentage of GFP+ cells stained by IHC and counted in MSS (left) and BSS (*right*) mouse tumors. d Example flow cytometry of mouse MSS (*left*) and BSS (*right*) for intrinsic GFP signaling in tumor cells and E-cadherin-APC. (Magnification bars =50 μm)

by immunohistochemistry by rehydrating slides through a citrosolv and ethanol dilution wash. Antigen-retrieval was performed in 10 mM sodium citrate (pH 6.0). Slides were blocked in 5% normal goat serum/0.3% Triton X-100/phosphate buffered saline, immunostained with anti-GFP antibody (Santa Cruz Biotechnologies, sc-8334, Santa Cruz, CA, USA), detected by horse radish peroxidase and hematoxylin counterstained. Light photomicrographs were obtained with an Olympus BX43 microscope and DP26 camera (Olympus America, Center Valley, PA, USA). From the mouse tumors, we cannot know whether the specific tumor segment that was dissociated and cultured was monophasic or biphasic. Because the bulk of each tumor was divided between snap frozen and culture samples, only the periphery of the tumors with their invasion into the surrounding host tissues are processed for histology. These analyses demonstrated monophasic synovial sarcoma histology for each specimen, but we know that approximately half of tumors in these mice likely had biphasic areas in the core of the tumor as well. Both human tumors were monophasic synovial sarcomas.

Flow Cytometry

Primary tumors were minced, and single cell suspensions generated using enzymatic and mechanical dissociation (Tumor Dissociation Kit and GentleMACS Tissue Homogenizer, Miltenyi Biotec, San Diego, CA, USA). Cells were strained using 70 μm MACS Smart strainers (Miltenyi Biotec), washed with PBS and 0.5 mg/mL bovine serum albumin, and stained with (10 μL for 10^6 cells) E-caderin-APC (R&D Systems, FAB7481A, Minneapolis, MN, USA) and DAPI. Flow cytometry was performed on a BD Facs Canto instrument (BD Bioscience, San Jose, CA, USA), and analyzed using FlowJo 8.7.1. E-cadherin positivity was established

Fig. 2 Mouse and human synovial sarcoma transcriptional comparisons. **a** Heatmap demonstrating distribution of 10,833 and 8834 differentially expressed genes between tumors and cell lines from mice (*left*) and humans (*right*). **b** Venn diagrams showing significant overlapping genes between mouse (*above*) and human (*below*) samples, comparing cell lines to primary tumors. **c** Venn diagram showing 2-fold change overlapping genes shared as different in the same direction between the two primary tumor to xenograft comparisons from human tumors. **d** Hierarchal clustering of primary tumor and cell line transcriptome profiles for mouse and human samples, (left and right, respectively). T = primary tumor; C = cell line; X = xenograft
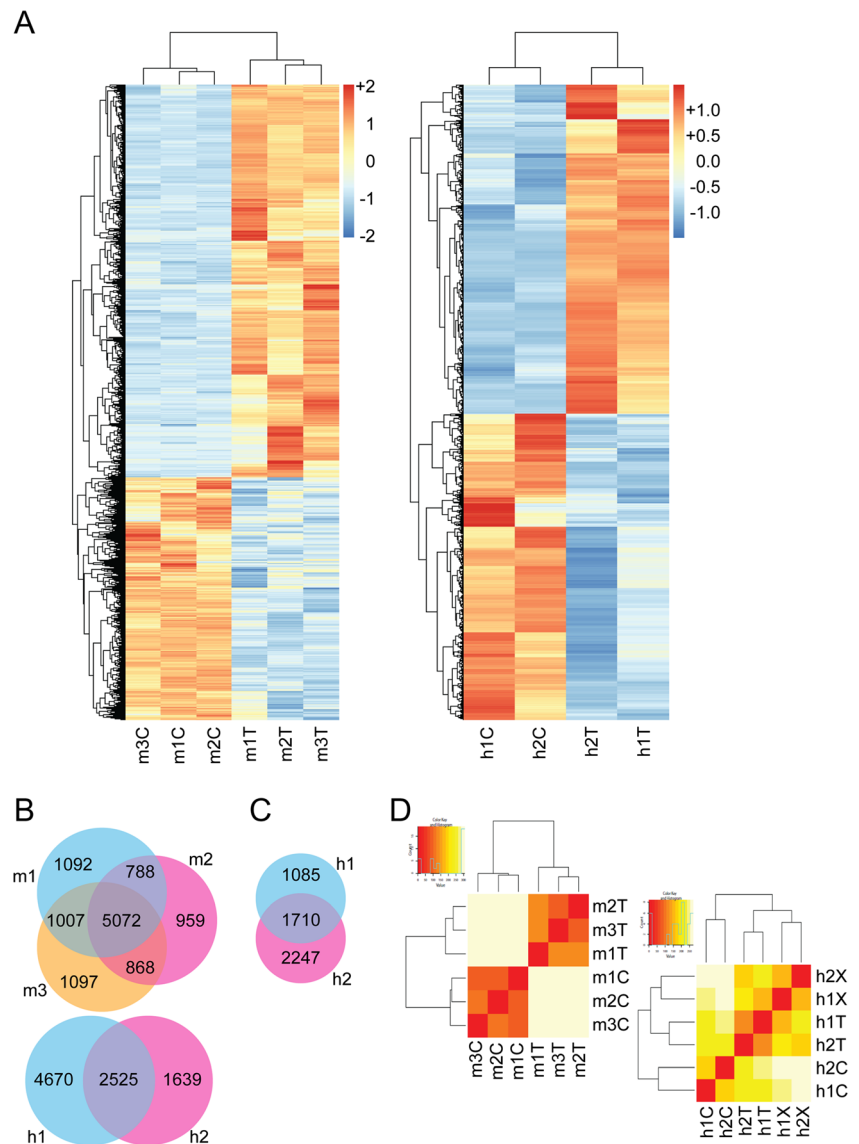
using a no antibody control sample. GFP is an intrinsically expressed fluorochrome and E-cadherin is a surface protein; thus, no permeabilization was required.

Cell Lines

Human cell lines were maintained in Dulbecco's modified eagle medium (DMEM) with 10% or 20% fetal bovine serum (FBS), and validated for the expression of and dependence (siRNA) on *SS18-SSX1*. The three mouse cell lines were similarly established and maintained in DMEM with 20% FBS. Each was validated for fusion gene expression by RT-PCR.

Results

To determine the composition of SSs developing in mice, we utilized the GFP reporter that is expressed with the SS18-SSX fusion. Immunohistochemistry against GFP identified greater than 90% of cells as stained in both histologic subtypes of SS, monophasic (only mesenchymal) and biphasic (including both mesenchymal and epithelial areas) (Fig. 1a-c).

A high fraction of tumor cells was also demonstrated by flow cytometry for GFP fluorescence (Fig. 1d). The slightly lower tumor cell fraction by flow cytometry was anticipated due to the relative filtering out of incompletely dissociated tumor cells embedded in matrix.

Table 1 IPA results from comparison between cell lines and native tumors

Ingenuity Canonical Pathways	-log(p-value)	Ratio	z-score
Mouse			
Hepatic Fibrosis / Hepatic Stellate Cell Activation	9.93E00	5.15E-01	
Agranulocyte Adhesion and Diapedesis	9.45E00	5.48E-01	
Calcium Signaling	8.73E00	5.1E-01	-5.060
Cellular Effects of Sildenafil (Viagra)	7.07E00	5.28E-01	
Crosstalk between Dendritic Cells and Natural Killer Cells	5.72E00	5.93E-01	
B Cell Development	5.58E00	7.73E-01	
Leukocyte Extravasation Signaling	5.36E00	4.44E-01	-1.697
Granulocyte Adhesion and Diapedesis	5.09E00	4.78E-01	
Eicosanoid Signaling	4.4E00	5.81E-01	-0.905
T Helper Cell Differentiation	4.35E00	5.62E-01	
Human			
Oxidative Phosphorylation	2.39E01	6.67E-01	
Mitochondrial Dysfunction	1.97E01	5.22E-01	
phagosome maturation	6.19E00	4.04E-01	
CD28 Signaling in T Helper Cells	5.09E00	3.89E-01	
Fcγ Receptor-mediated Phagocytosis in Macrophages and Monocytes	4.46E00	3.84E-01	-0.870
Complement System	4.23E00	5.36E-01	1.508
Dendritic Cell Maturation	3.97E00	3.36E-01	
Crosstalk between Dendritic Cells and Natural Killer Cells	3.33E00	3.93E-01	
Allograft Rejection Signaling	3.15E00	4.81E-01	
Altered T Cell and B Cell Signaling in Rheumatoid Arthritis	2.93E00	4E-01	
Combined mouse and human			
CD28 Signaling in T Helper Cells	3.52E00	1.63E-01	
B Cell Development	3.49E00	4.17E-01	
Serine Biosynthesis	3.16E00	7.5E-01	
Dendritic Cell Maturation	2.93E00	1.38E-01	
Oxidative Phosphorylation	2.87E00	1.54E-01	
Superpathway of Serine and Glycine Biosynthesis I	2.5E00	5E-01	
Complement System	2.47E00	2.63E-01	0.000
Phagosome maturation	2.42E00	1.36E-01	
FcγRIIB Signaling in B Lymphocytes	2.38E00	1.89E-01	1.134
PKCθ Signaling in T Lymphocytes	2.38E00	1.35E-01	2.714

Fig. 3 Pathways highlighted in genes differentially expressed between cell lines and tumors in synovial sarcoma. Results of quantitative IPA analysis
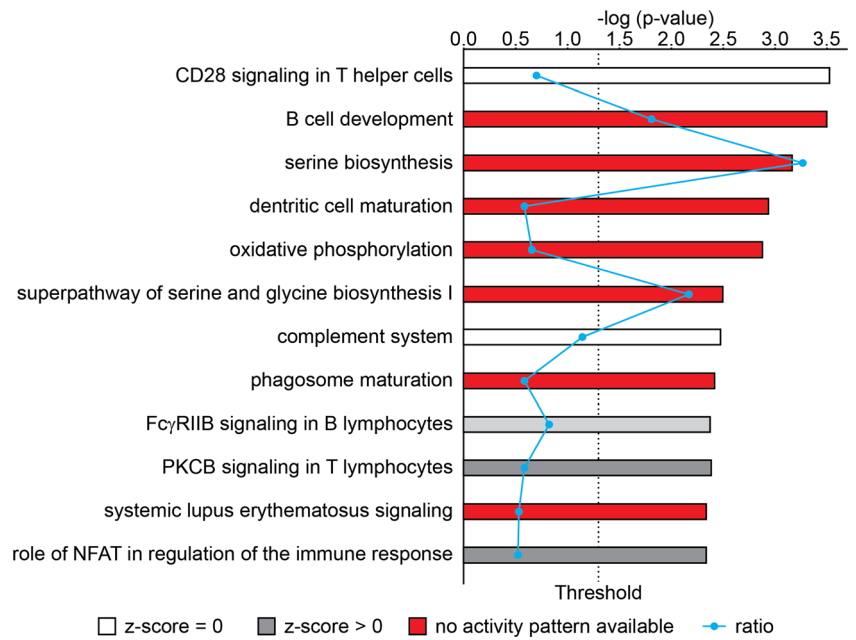
Freshly harvested SSs from the mice were divided into samples for snap freezing to enable subsequent total RNA procurement and for immediate dissociation and culture. Of 6 attempts at culture, 3 successfully generated passageable cell lines that retained SS18-SSX expression.

Freshly harvested human SSs were divided into 3 samples each, for snap freezing, dissociation and culturing, and immediate xenograft implantation into NSG mice. The success rate of generating passageable cell lines was only 2 of 10, but both of these primary tumors also grew as xenograft implantations. Histology of other samples from the two tumors that grew demonstrated monophasic SSs, with very high percentage of apparent tumor cells.

Transcriptome sequencing revealed a large number of genes (10,883 for mouse, and 8834 for human) to be differentially expressed by at least 2-fold and $p < 0.05$ significance in cell lines compared to the original tumors. Heatmaps revealed that in both mouse and human pairs, differentially expressed genes shared directional changes in each tumor-cell comparison (Fig. 2a). Venn diagram analysis demonstrated 5072 out of 10,883 total altered genes were shared at the same level of stringency in all three tumor-cell comparisons in the mouse (Fig. 2b). The two human comparisons shared 2525 out of 8834 (Fig. 2b). Hierarchical cluster analysis segregated cell lines from tumors (Fig. 2c). Ingenuity Pathway Analysis (IPA) found that differentially expressed genes associated with multiple pathways (Table 1), but highlighted inflammatory infiltrates and metabolism (Fig. 3 and Table 1).

We next tested if the transcriptional shift in cultured cells could be rescued by the xenograft environment. Hierarchal clustering of human cell lines, xenografted tumors, and primary tumors more closely associated the latter two (Fig. 2c). The yet differentially expressed genes most prominently featured metabolism (Table 2).

Table 2 IPA results comparing native to xenografted human tumors

Ingenuity Canonical Pathways	-log(p-value)	Ratio	z-scor.
Phosphatidylethanolamine Biosynthesis II	2.55E00	6.25E-01	
Sperm Motility	2.35E00	2.65E-01	-0.728
Glioma Invasiveness Signaling	1.74E00	2.69E-01	0.000
Phospholipases	1.69E00	2.89E-01	
BER pathway	1.62E00	4.17E-01	
phagosome formation	1.56E00	2.33E-01	
Triacylglycerol Degradation	1.47E00	3.85E-01	
Reelin Signaling in Neurons	1.46E00	2.36E-01	
Production of NO and Reactive Oxygen Species in Macrophages	1.44E00	2.07E-01	-2.335
Lipid Antigen Presentation by CD1	1.33E00	3.57E-01	

Discussion

There is an on-going debate about what constitutes the most appropriate preclinical model for the study of cancer. Our data are not the first to indicate that cell lines fail in some respects to recapitulate tumor biology. In a prior study, only 34 of 60 cancer cell line expression profiles reflected well the tumor types they represented [11]. Here, transcriptome data from 3 mouse and 2 human SS tumor-to-cell line matched pairs identified broad deviations, but mostly related to the microenvironment, such as inflammatory infiltrates and metabolism.

Prior transcriptome profiling work has described gene expression patterns shared across various SS cases. Highlighted genes have included those involved in epithelial differentiation (such as ERBB2, IGFBP2/3 and EGFR), neural differentiation (such as neurofilament, ephrinB3 and EphA4), and tumor markers (TLE1, Keratin, etc.) [12–15]. Our analyses found few alterations in the expression of these core genes (except for ephrin pathway genes, see Table 1). This suggests that SS-derived cells in culture largely maintain the "molecular signature" of SS tumors and that expression of these signature genes is regulated by intrinsic transcriptional regulatory programs that function independently from culture or in vivo conditions.

Our data revealed considerable variation in gene expression profiles overall and the enrichment of microenvironment modification-related genes among those differentially expressed genes across all examined tumor-to-cell line comparisons. Among the most differentially regulated genes are those related to inflammatory infiltrates and metabolism (Fig. 3), indicating cellular heterogeneity and interactions as well as energy/nutrition conditions may play a critical role in gene expression in SS tumors. While we hoped to be able to distinguish the contributions from infiltrating cells in the xenografted human tumors, complete exclusion of transcriptomic contributions from murine infiltrating cells is impossible due to the strong homology between mouse and human coding sequences. Further, while tumor infiltrating lymphocytes are rare in synovial sarcomas, they would be especially rare in the immune compromised host mice for xenografts.

Because much of drug discovery work begins in cell lines, as the science pertinent to the interaction of the microenvironment and drug responses develops, we should bear in mind the magnitude of its impacts even on tumors with relatively strong homogeneity and few stromal and immune infiltrates.

Compliance with Ethical Standards

Conflict of Interest The authors declare that they have no conflict of interest.

Ethical Approval All procedures performed in studies involving human participants were in accordance with the ethical standards of the institutional research committee and with the 1964 Helsinki declaration and its later amendments or comparable ethical standards. All procedures performed in studies involving animals were in accordance with the ethical standards of the institution at which the studies were conducted. All applicable international, national, and/or institutional guidelines for the care and use of animals were followed.

Informed Consent Informed consent was obtained from all individual participants included in the study.

References

1. Begley CG, Ellis LM (2012) Drug development: raise standards for preclinical cancer research. Nature 483(7391):531–533

2. Herzog CE (2005) Overview of sarcomas in the adolescent and young adult population. J Pediatr Hematol Oncol 27(4):215–218

3. Vlenterie M, Litiere S, Rizzo E, Marreaud S, Judson I, Gelderblom H, Le Cesne A, Wardelmann E, Messiou C, Gronchi A, van der Graaf WT (2016) Outcome of chemotherapy in advanced synovial sarcoma patients: review of 15 clinical trials from the European Organisation for Research and Treatment of Cancer soft tissue and bone sarcoma group; setting a new landmark for studies in this entity. Eur J Cancer 58:62–72

4. Jones KB, Barrott JJ, Xie M, Haldar M, Jin H, Zhu JF, Monument MJ, Mosbruger TL, Langer EM, Randall RL, Wilson RK, Cairns BR, Ding L, Capecchi MR (2016) The impact of chromosomal translocation locus and fusion oncogene coding sequence in synovial sarcomagenesis. Oncogene 35:5021–5032

5. Clark J, Rocques PJ, Crew AJ, Gill S, Shipley J, Chan AM, Gusterson BA, Cooper CS (1994) Identification of novel genes, SYT and SSX, involved in the t(X;18)(p11.2;q11.2) translocation found in human synovial sarcoma. Nat Genet 7(4):502–508

6. de Leeuw B, Balemans M, Olde Weghuis D (1995) Geurts van Kessel a. Identification of two alternative fusion genes, SYT-SSX1 and SYT-SSX2, in t(X;18)(p11.2;q11.2)-positive synovial sarcomas. Hum Mol Genet 4(6):1097–1099

7. Kottu R, Prayaga AK (2010) Synovial sarcoma with relevant immunocytochemistry and special emphasis on the monophasic fibrous variant. J Cytol 27(2):47–50

8. Sherr CJ, DePinho RA (2000) Cellular senescence: mitotic clock or culture shock? Cell 102(4):407–410

9. Benjamini Y, Hochberg Y (1995) Controlling the false discovery rate: a practical and powerful approach to multiple testing. J R Stat Soc 57(1):289–300

10. Ching T, Huang S, Garmire LS (2014) Power analysis and sample size estimation for RNA-Seq differential expression. RNA 20(11): 1684–1696

11. Sandberg R, Ernberg I (2005) Assessment of tumor characteristic gene expression in cell lines using a tissue similarity index (TSI). Proc Natl Acad Sci U S A 102(6):2052–2057

12. Nagayama S, Katagiri T, Tsunoda T, Hosaka T, Nakashima Y, Araki N, Kusuzaki K, Nakayama T, Tsuboyama T, Nakamura T, Imamura M, Nakamura Y, Toguchida J (2002) Genome-wide analysis of gene expression in synovial sarcomas using a cDNA microarray. Cancer Res 62(20):5859–5866

13. Allander SV, Illei PB, Chen Y, Antonescu CR, Bittner M, Ladanyi M, Meltzer PS (2002) Expression profiling of synovial sarcoma by cDNA microarrays: association of ERBB2, IGFBP2, and ELF3 with epithelial differentiation. Am J Pathol 161(5):1587–1595

14. Fernebro J, Francis P, Eden P, Borg A, Panagopoulos I, Mertens F, Vallon-Christersson J, Akerman M, Rydholm A, Bauer HC, Mandahl N, Nilbert M (2006) Gene expression profiles relate to SS18/SSX fusion type in synovial sarcoma. Int J Cancer 118(5):1165–1172

15. Ross DT, Scherf U, Eisen MB, Perou CM, Rees C, Spellman P, Iyer V, Jeffrey SS, Van de Rijn M, Waltham M, Pergamenschikov A, Lee JC, Lashkari D, Shalon D, Myers TG, Weinstein JN, Botstein D, Brown PO (2000) Systematic variation in gene expression patterns in human cancer cell lines. Nat Genet 24(3):227–235